


Sound velocities of skiagite–iron–majorite solid solution to 56 GPa probed by nuclear inelastic scattering

D. M. Vasiukov^{1,2}  · L. Ismailova³ · I. Kupenko⁴ · V. Cerantola⁵ · R. Sinmyo² · K. Glazyrin⁶ · C. McCammon² · A. I. Chumakov⁵ · L. Dubrovinsky² · N. Dubrovinskaia¹

Received: 22 July 2017 / Accepted: 31 October 2017 / Published online: 10 November 2017
© Springer-Verlag GmbH Germany 2017

Abstract High-pressure experimental data on sound velocities of garnets are used for interpretation of seismological data related to the Earth's upper mantle and the mantle transition zone. We have carried out a Nuclear Inelastic Scattering study of iron-silicate garnet with skiagite (77 mol%)–iron–majorite composition in a diamond anvil cell up to 56 GPa at room temperature. The determined sound velocities are considerably lower than sound velocities of a number of silicate garnet end-members, such as grossular, pyrope, Mg–majorite, andradite, and almandine. The obtained sound velocities have the following pressure dependencies: V_p [km/s] = 7.43(9) + 0.039(4) × P [GPa] and V_s [km/s] = 3.56(12) + 0.012(6) × P [GPa]. We estimated sound velocities of pure skiagite and khoharite, and conclude that the presence of the iron–majorite component in skiagite strongly decreases V_s . We analysed the influence of

Fe³⁺ on sound velocities of garnet solid solution relevant to the mantle transition zone and consider that it may reduce sound velocities up to 1% relative to compositions with only Fe²⁺ in the cubic site.

Keywords Nuclear inelastic scattering · Sound velocities · Skiagite · Khoharite · Garnet · Mantle transition zone

Introduction

Garnets are an abundant group of minerals that are stable down to the top of the lower mantle (~ 720 km). Their elastic properties are important for interpretation of seismological data as they constitute a substantial part of the upper mantle and mantle transition zone (MTZ). The fraction of garnet in peridotite and eclogite assemblages can increase up to 35 and 95 vol%, respectively, at MTZ conditions as pyroxenes progressively dissolve in garnet with increasing depth (Irifune and Ringwood 1993; Irifune et al. 1986; Litasov and Ohtani 2005; Ricolleau et al. 2010; Ringwood 1991; Wood et al. 2013).

Silicate garnets have the general formula $X_3^{2+} Y_2^{3+} (\text{SiO}_4)_3$ and crystallize in a cubic structure (space group $Ia\bar{3}d$, Fig. 1). The distorted cubic site (X-site) is occupied by large divalent cations (Mg, Fe, Ca, Mn), while the octahedral site (Y-site) is populated by trivalent (Al, Fe, Cr) cations. Pyroxene dissolution in garnet at high-pressure high-temperature (HPHT) conditions leads to an excess of silicon that is incorporated in the Y-site. In such garnets, Si⁴⁺ is balanced either by divalent cations in the Y-site [mainly Mg, Mg₃(Mg,Si)(SiO₄)₃] or by sodium in the X-site [(Na₂,Mg)Si₂(SiO₄)₃]. Therefore, the presence of such a majorite component is an unambiguous indication of a high-pressure formation of the garnet.

Electronic supplementary material The online version of this article (<https://doi.org/10.1007/s00269-017-0928-8>) contains supplementary material, which is available to authorized users.

✉ D. M. Vasiukov
vasyukov@physics.msu.ru

- ¹ Laboratory of Crystallography, Universität Bayreuth, Universitätsstr. 30, 95447 Bayreuth, Germany
- ² Bayerisches Geoinstitut, Universität Bayreuth, Universitätsstr. 30, 95447 Bayreuth, Germany
- ³ Skolkovo Innovation Center, Skolkovo Institute of Science and Technology, ul. Nobelya 3, Moscow 143026, Russia
- ⁴ Institut für Mineralogie, Universität Münster, Corrensstr. 24, 48149 Münster, Germany
- ⁵ ESRF-The European Synchrotron, CS40220, 38043 Grenoble Cedex 9, France
- ⁶ Photon Science, Deutsches Elektronen-Synchrotron, Notkestr. 85, 22603 Hamburg, Germany

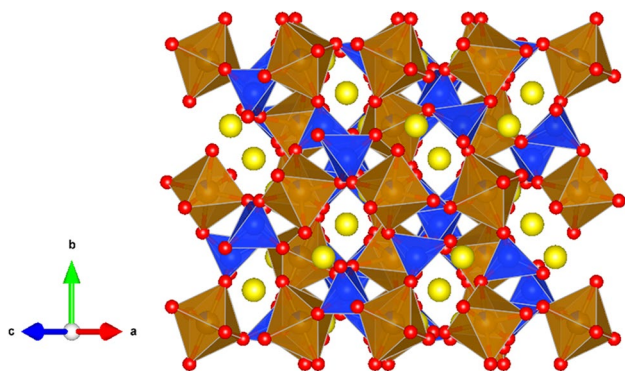


Fig. 1 Crystal structure of skiaegite–Fe–majorite solid solution. The corner-shared alternating Si tetrahedra (Z-site) and (Fe, Si)-octahedra (Y-site) form a framework in the garnet structure. The distorted cubic voids (X-site) are populated by divalent iron (depicted as yellow isolated atoms). The structure is visualized using the VESTA software (Momma and Izumi 2011)

Up until now, HPHT studies of the elastic properties of garnets have focused on the end-members with Mg, Ca, and Fe^{2+} populating the X-site and Al, (Mg, Si) on the Y-site (Arimoto et al. 2015; Chantel et al. 2016; Gwanmesia et al. 2014; Kono et al. 2010; Zhou et al. 2014; Zou et al. 2012). However, there is strong evidence to support the hypothesis of reducing conditions and stabilization of Fe–Ni alloy below 250 km depth (Rohrbach et al. 2007; Woodland and Koch 2003), so one should consider the disproportionation reaction $\text{Fe}^{2+} \rightarrow \text{Fe}^{3+} + \text{Fe}^0$ and a subsequent incorporation of ferric iron into garnet. Recently, highly oxidized majoritic inclusions from deep mantle xenoliths were found (Xu et al. 2017) and majoritic inclusions from deep mantle diamonds (Kiseeva et al. 2017, accepted) revealed that the amount of Fe^{3+} in the Y-site increases considerably with depth (up to 25–30% of total iron at 500 km). These data indicate that garnets such as andradite [$\text{Ca}_3\text{Fe}_2(\text{SiO}_4)_3$] and skiaegite [$\text{Fe}_3^{2+}\text{Fe}_2^{3+}(\text{SiO}_4)_3$] are potentially important for the Earth's upper mantle and MTZ.

Here, we present an experimental high-pressure study of skiaegite–iron–majorite [$\text{Fe}_3(\text{Fe}^{2+}, \text{Si})(\text{SiO}_4)_3$] solid solution in a diamond anvil cell (DAC) at room temperature using Nuclear Inelastic Scattering (NIS, also known as NRIXS—Nuclear Resonant Inelastic X-ray Scattering).

Experimental methods

The single crystals of skiaegite–iron–majorite were synthesized in a multi-anvil apparatus at 9.5 GPa and 1100 °C from a powdered mixture of chemically pure oxides Fe_{1-x}O , $^{57}\text{Fe}_2\text{O}_3$ and SiO_2 (Ismailova et al. 2015). The material that we studied has composition $\text{Fe}_3^{2+}[\text{Fe}_{1.532(2)}^{3+}\text{Fe}_{0.234(2)}^{2+}\text{Si}_{0.234(2)}](\text{SiO}_4)_3$ based on

single-crystal X-ray diffraction and microprobe analysis (Ismailova et al. 2015), and therefore, the samples contain approximately 23 mol% of iron–majorite component. High-quality crystals were selected based on the quality of their diffraction peak profiles using a three-circle Bruker diffractometer equipped with a SMART APEX CCD detector and a high-brilliance Rigaku rotating anode (Rotor Flex FR-D, Mo- K_α radiation) with Osmic focusing X-ray optics.

For pressure generation, we used panoramic DACs designed and manufactured in Bayerisches Geoinstitut. The size of the diamond culets was 250 μm . The isometric crystals of the garnet with typical linear dimension of $\sim 15 \mu\text{m}$ and a small ruby sphere were loaded into the pressure chamber in beryllium gaskets (the indentation thickness and the hole diameter were 30 and 120 μm , respectively). Several garnet crystals were loaded, and all measurements except the one at 56 GPa were performed on the single crystal that gave the strongest NIS signal. The data point at 56 GPa was collected from another garnet crystal in a separate another DAC. Neon was used as pressure transmitting medium. Pressure in the DAC was determined by ruby fluorescence (Dewaele et al. 2008). It was measured before and after each data collection and the average value was used.

The single-crystal NIS experiments were performed at ambient temperature at the Nuclear Resonance Beamline (ID18, Ruffer and Chumakov 1996) of the European Synchrotron Radiation Facility. The synchrotron ring was operated in hybrid mode (one clean 4 mA single bunch diametrically opposed to a ~ 196 mA multi-bunch beam composed of 24 groups of bunches spread over 3/4 of the storage ring circumference). The data were collected at ambient temperature over a range of -20 to 100 meV relative to the ^{57}Fe nuclear resonance energy (14.4 keV) with 0.5 meV step. The energy bandwidth and the beam spot size were 2.3 meV and $7 \times 13 \mu\text{m}^2$, respectively. The data were processed using the DOS software (Kohn and Chumakov 2000).

Experimental results

The NIS technique provides information about lattice dynamics via nuclear resonant inelastic absorption and has its roots in the Mössbauer effect (see Chumakov and Ruffer 1998 for a review of the development of the method). The NIS spectrum consists of the elastic (the recoilless absorption, i.e., the Mössbauer effect) and inelastic part (which appears due to inelastic interactions with phonons in the studied sample). Data processing involves removal of the elastic peak and subtraction of background multi-phonon contributions, followed by determination of the partial (atomic) phonon density of states (pDOS). The raw NIS

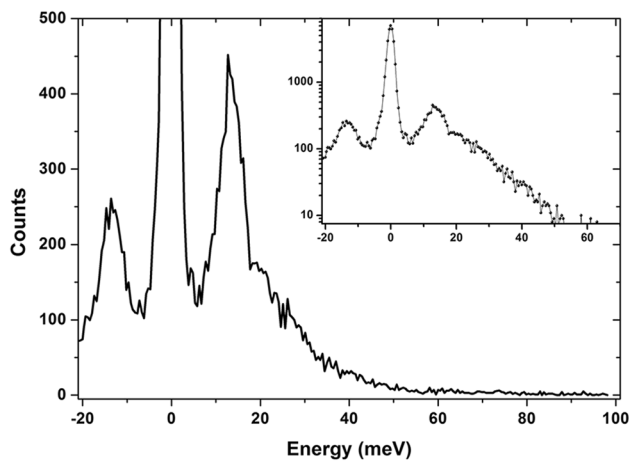


Fig. 2 Raw NIS spectrum of skiaigite–iron–majorite solid solution at ambient conditions. The elastic peak at 0 meV is surrounded by phonon creation (positive energy) and annihilation (negative energy) wings. The inset shows the same spectrum in logarithmic scale

spectrum of the studied solid solution at ambient conditions is shown in Fig. 2 (for pressure evolution of the NIS spectra, see the Supplementary Information). A visual illustration of all the main steps in NIS data analysis can be found in Hu et al. (1999). For the detailed mathematical treatment, the reader is referred to Kohn et al. (1998).

Partial phonon density of states

Garnet has four formula units (80 atoms) per primitive unit cell. The phonon density of states (DOS) of garnet is, therefore, related to 240 vibrational branches. Garnet has a phonon bandgap between 80 and 100 meV and the high-energy band is composed of 48 modes mainly related to the vibrations of tetrahedral subunit (Baima et al. 2016; Mittal et al. 2001; Papagelis et al. 2002). The measured iron pDOS (Fig. 3), therefore, consists of 192 vibrational branches (3 acoustic and 189 optical).

The studied crystals have cubic symmetry; therefore, the obtained pDOS does not have directional dependence (Kohn et al. 1998) and represents the average pDOS of the crystal, not the projected one. The thermodynamic and vibrational parameters extracted from the iron pDOS are presented in Table 1. Because iron populates two crystallographic sites (X and Y), the parameters are the averaged values in the first approximation. However, it is not an exact averaging, because contributions of the X- and Y-sites are weighted by the corresponding Lamb–Mössbauer factors which are distinct (see discussion in Sturhahn and Chumakov 1999).

So far, there has been no theoretical investigation of the phonon properties of skiaigite or iron–majorite. Nevertheless, the contributions of the different crystallographic sites to the iron pDOS at ambient conditions (Fig. 4) can be assigned using

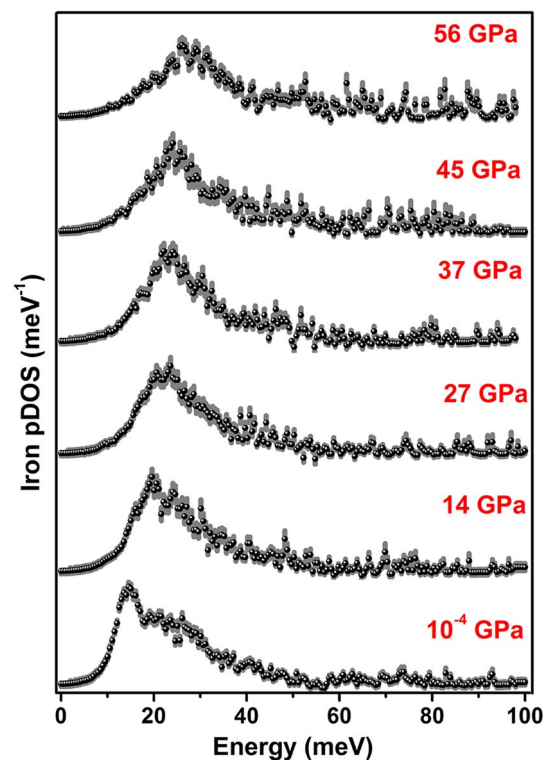


Fig. 3 Pressure evolution of the extracted pDOS. Vertical grey bars are the standard deviations

the theoretical iron pDOS of almandine [$\text{Fe}_3\text{Al}_2(\text{SiO}_4)_3$] and/or andradite. This is possible, because the potential wells of the X- and Y-sites in skiaigite–iron–majorite solid solutions should be similar to those of X-site Fe^{2+} in almandine and Y-site Fe^{3+} in andradite, respectively. Hence, this approach is also valid for the iron pDOS. In the literature, only the pDOS of X-site Fe^{2+} in almandine has been reported (Mittal et al. 2000, 2001) as obtained from semi-empirical interatomic potential calculations. Comparing it with our experimental iron pDOS (Fig. 4), one can judge that the 15 meV peak is dominated by vibrations of X-site Fe^{2+} . Accordingly, after subtracting the X-site contribution from experimental pDOS, one can see that the noticeable contribution of Y-site Fe appears above 18 meV and the low-intensity 55–80 meV band is formed only by its vibrations.

Sound velocities

The determination of the sound velocities from the NIS data is based on the evaluation of the Debye sound velocity from the low-energy part of the pDOS (Hu et al. 2003). The latter depends quadratically on the energy and can be written in the following form (Achterhold et al. 2002; Hu et al. 2003):

$$D(E) = \left(\frac{\tilde{m}}{m}\right) \frac{E^2}{2\pi^2 \hbar^3 n V_D^3}, \quad (1)$$

Table 1 Extracted parameters from the NIS spectra and elastic moduli of skiaite–iron–majorite solid solution

Pressure (GPa)	Lamb-Mössbauer factor	Vibrational amplitude (Å)	Mean internal energy (meV)	Specific heat (k_B /atom)	Entropy (k_B /atom)	Norm. mean force constant (N/m)	Debye velocity (km/s)	Isothermal bulk modulus (GPa)	Shear modulus (GPa)	Poisson's ratio
10^{-4}	0.710 (3)	0.1389 (3)	85.0 (2)	2.705 (7)	3.50 (3)	201 (4)	3.97 (14)	160 (5)	57 (4)	0.34
14 (1)	0.78 (1)	0.120 (3)	87 (1)	2.65 (2)	3.1 (1)	240 (20)	4.3 (2)	218 (2)	72 (7)	0.35
27 (1)	0.80 (1)	0.114 (3)	88 (1)	2.62 (2)	3.0 (1)	260 (30)	4.5 (3)	268 (3)	82 (10)	0.36
37 (1)	0.80 (1)	0.114 (3)	87 (1)	2.63 (2)	3.0 (1)	250 (30)	4.3 (3)	304 (5)	77 (11)	0.38
45 (2)	0.82 (1)	0.107 (3)	90 (1)	2.55 (2)	2.8 (1)	320 (30)	4.7 (4)	334 (7)	96 (17)	0.37
56 (3)	0.84 (1)	0.101 (3)	94 (1)	2.44 (2)	2.5 (1)	420 (40)	4.8 (5)	–	–	–

These parameters are “averaged” values for the two crystallographic sites (see main text). The isothermal bulk moduli were taken from (Ismailova et al. 2017)

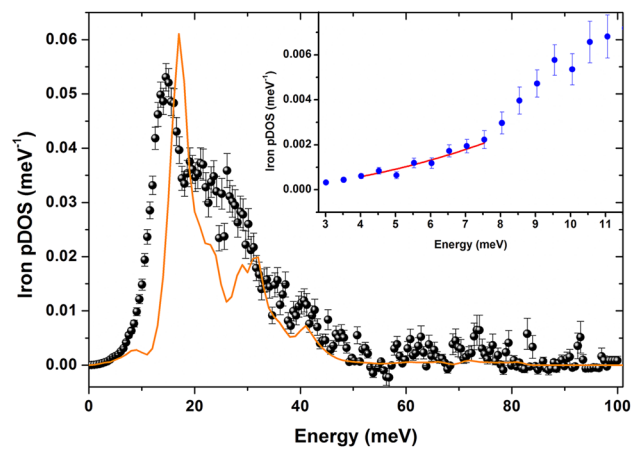


Fig. 4 Iron pDOS of skiaite–iron–majorite solid solution at ambient conditions. The yellow line is the calculated pDOS of X-site Fe^{2+} in almandine (Mittal et al. 2000). Comparing it with our experimental pDOS, one can judge that the 15 meV peak is dominated by vibrations of X-site Fe^{2+} . The dip on the almandine pDOS around 11 meV is a calculation artefact; see Fe pDOS in a subsequent paper of the same group (Mittal et al. 2001). The inset shows the example of the parabolic fit for the low-energy part of the experimental pDOS at 27 GPa

where \tilde{m} is the mass of the nuclear resonant isotope (^{57}Fe in our case), m is the average atomic mass, n is the density of atoms, and V_D is Debye sound velocity.

Due to the small size of the garnet Brillouin zone, the acoustic modes can cross with optical modes even below 10 meV at ambient conditions (Baima et al. 2016; Papagelis et al. 2002). This leads to a narrow range for the parabolic fit of the low-energy part of pDOS, and thus, we carried it out from 4 to 7–10 meV depending on the pressure (Fig. 4). The data below 4 meV lie under the strong elastic peak in the NIS spectrum, so data points affected by the elastic peak subtraction are not used for the fitting. The upper limit of the fitted interval is determined by the deviation of the pDOS data from parabolic dependence. The phonon spectrum shifts to higher energies with increasing pressure, so the parabolic region is extended at higher pressures.

The Debye sound velocity can be expressed as follows:

$$\frac{3}{V_D^3} = \frac{1}{V_p^3} + \frac{2}{V_s^3}, \quad (2)$$

where V_p is the average velocity of the *primary* (compression) wave and V_s is the average velocity of the *secondary* (shear) wave. There is additional relationship between V_p and V_s :

$$V_p = \sqrt{\frac{K + 4/3G}{\rho}}, \quad V_s = \sqrt{\frac{G}{\rho}} \quad (3)$$

$$\Rightarrow \frac{K}{\rho} = V_k^2 = V_p^2 - \frac{4}{3}V_s^2,$$

where K is the adiabatic bulk modulus, G is the shear modulus, and ρ is the density. The density was determined using the equation of state (EoS) from Ismailova et al. (2017), which was measured on the same material that we studied. Besides, the isothermal bulk modulus K_T was used instead of adiabatic bulk modulus (Table 1). The latter introduces a negligible error, as K_T is only slightly lower than K at ambient temperature (for example, for andradite, the difference is 0.7%, Jiang et al. 2004).

Generally speaking, the equations (1), (2), (3) are valid for elastically isotropic media. The use of them is justified, as garnets have very small elastic anisotropy (Erba et al. 2014). The system of Eqs. (2) and (3) has an approximate solution according to the corrected formula from Sturhahn and Jackson (2007):

$$V_p = \sqrt{1.002V_k^2 - 0.104V_kV_D + 1.208V_D^2},$$

$$V_s = 0.952V_D - 0.041V_k. \tag{4}$$

Figure 5 shows the obtained values of V_p and V_s as function of pressure. For the data point at 56 GPa, we report only Debye sound velocity (Table 1) as the bulk modulus of the sample is unknown due to the spin crossover of Y-site octahedral iron in this pressure range (Ismailova et al. 2017). A linear fit gives the following pressure dependencies of sound velocities at ambient temperature:

$$V_p = 7.43(9) + 0.039(4) \times P, \quad V_s = 3.56(12) + 0.012(6) \times P. \tag{5}$$

Here, V_p and V_s are in km/s and pressure is in GPa. The magnitudes of sound velocities are substantially lower than for all other garnet end-members considered so far, while

the pressure derivatives of both V_p and V_s are comparable (Fig. 5).

Discussion

In petrological models of the upper mantle and MTZ, iron ions are conventionally assumed to be divalent. This is also a common assumption when reducing electron microprobe data of natural samples from the deep mantle. In the case of garnet, Fe^{2+} is assigned to the X-site. It is, therefore, important to estimate the extent to which the presence of Fe in the Y-site can influence sound velocities of the complex garnet solid solution. The most important consequences would be for the seismic profile in the 400–600 km depth interval where pyroxene completely dissolves into garnet and the volume fraction of the latter reaches a maximum (Wood et al. 2013).

Experimental studies have shown that, in the presence of both Mg and Fe in the majorite solid solution, there is a strong preference to balance Si^{4+} in the Y-site by Mg^{2+} (not Fe^{2+}) (Kiseeva et al. 2017, accepted; McCammon and Ross 2003). Moreover, in the presence of Al, Fe^{2+} was not detected in the Y-site at all. Therefore, for further discussion, only end-members with ferric iron in the octahedral site are important.

Garnets with Y-site Fe^{3+} : skiaigite and khoharite

Among garnets of interest, only the elastic properties of andradite have been studied in detail (Jiang et al. 2004).

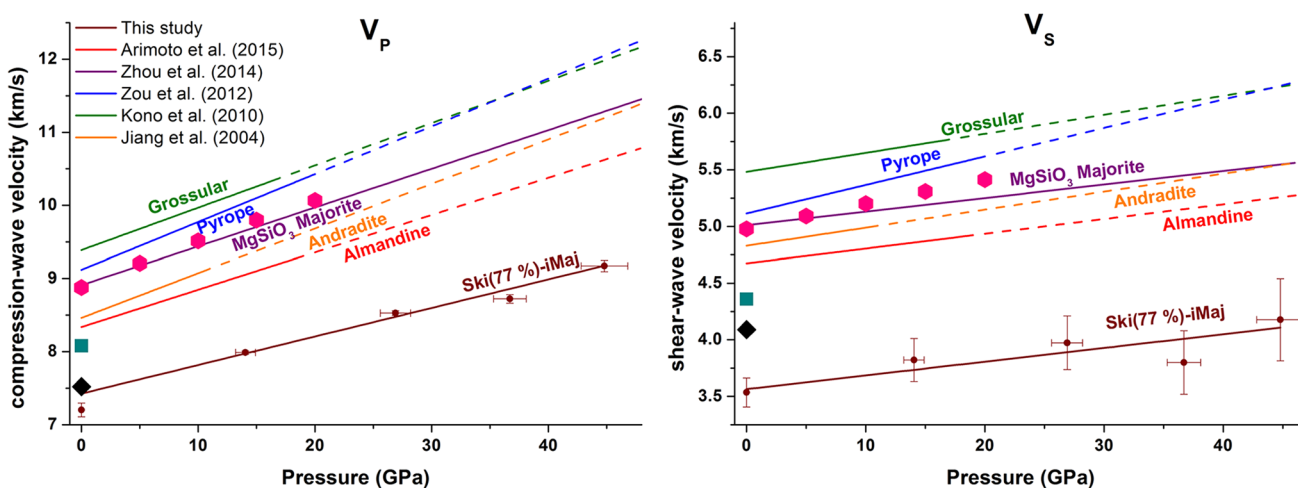


Fig. 5 Sound velocities of skiaigite–iron–majorite solid solution and some silicate garnet end-members as a function of pressure at ambient temperature. The black diamonds, cyan squares, and pink hexagons are estimated sound velocities of pure skiaigite, khoharite, and

JF-55A inclusion (correct composition with Y-site Fe^{3+}), respectively (see main text). The solid lines conform to the pressure range investigated in the corresponding studies, while dashed lines designate regions of extrapolation

Due to the lack of experimental data for pure skiaigite, we will estimate its elastic moduli based on solid solution considerations.

For a solid solution formed by atomic substitution on multiple distinct crystallographic sites, the unknown elastic moduli and sound velocities of end-members can be estimated from solid solutions with a particular composition. Let us consider the hypothetical solid solution $(\text{Fe}_{2.4}\text{Ca}_{0.6})(\text{Fe}_{0.4}\text{Al}_{1.6})(\text{SiO}_4)_3$ for the estimation of sound velocities of pure skiaigite. The composition has two equivalent representations using end-members: 20% And + 80% Alm \equiv 20% Gro + 20% Ski + 60% Alm [Gro refers to grossular— $\text{Ca}_3\text{Al}_2(\text{SiO}_4)_3$]. From Fig. 5 and a comparison of sound velocities of these end-members, one can see that the first representation should lead to sound velocities higher than almandine lines. As the second representation is equivalent, it is obvious that skiaigite should balance grossular relative to the almandine line.

Assuming the validity of Vegard's law, we obtain $a = 11.73 \text{ \AA}$ for pure skiaigite (unit cell parameters of almandine, andradite, and grossular were taken from Arimoto et al. (2015), Jiang et al. (2004), and Rodehorst et al. (2002), respectively). The unit cell parameter is in excellent agreement with experimental data (11.73 \AA , Woodland et al. 1999; Woodland and Ross 1994).

A widely used assumption for the pyralspite (pyrope–almandine–spessartine) series (Erba et al. 2014) is that elastic moduli of the solid solution depend linearly on those of the end-members. A recent ab initio investigation verified this assumption for the grossular–andradite solid solution (Lacivita et al. 2014). Using this assumption for skiaigite gives an aggregate adiabatic bulk modulus of 156.6 GPa, a shear modulus of 76.4 GPa, and Poisson's ratio of 0.29. For these calculations, we used the aggregate elastic moduli known from the literature for almandine (Arimoto et al. 2015) and andradite (Jiang et al. 2004), as well as the average of values for grossular published by Kono et al. (2010) and Gwanmesia et al. (2014). The calculated bulk modulus is in good agreement with the experimental isothermal bulk modulus of 157(3) GPa (Woodland et al. 1999); hence, we consider our approximation to be valid and use the calculated moduli to obtain the values $V_p = 7.52 \text{ km/s}$ and $V_s = 4.09 \text{ km/s}$ for skiaigite at ambient conditions (plotted in Fig. 5 as black diamonds). Comparing our experimental data of skiaigite–iron–majorite solid solution and estimated sound velocities of pure skiaigite (Fig. 5), one can see that the presence of iron–majorite strongly decreases V_s . This fact suggests non-linear behavior for the studied solid solution (the isothermal bulk modulus values also show non-linear behavior for this composition, see Ismailova et al. 2017). The cause of this behavior requires further investigation.

Recently reported majoritic inclusions in host garnet from an eclogite xenolith (Xu et al. 2017) contain a considerable

amount (from 40 to 48% depending on the particular end-member representation) of khoharite, $\text{Mg}_3\text{Fe}_2(\text{SiO}_4)_3$. This Y-site Fe^{3+} end-member may, therefore, also be relevant for the Earth's mantle. However, there are no experimental data at all for this garnet; only a single theoretical study (Milman et al. 2001).

We can estimate khoharite sound velocities in a similar way as performed above for skiaigite. The hypothetical solid solution with composition $(\text{Mg}_{2.4}\text{Ca}_{0.6})(\text{Al}_{1.6}\text{Fe}_{0.4})(\text{SiO}_4)_3$ can be represented as 20% And + 80% Pyr \equiv 20% Gro + 20% Kho + 60% Pyr [Pyr refers to pyrope— $\text{Mg}_3\text{Al}_2(\text{SiO}_4)_3$]. Elastic moduli and the unit cell parameter of pyrope were taken from Chantel et al. (2016) (results of “global” fit) and Hazen and Finger (1978), respectively. We obtain the following values for khoharite: $a = 11.66 \text{ \AA}$, $\rho = 3.859 \text{ g/cm}^3$, $K = 153.9 \text{ GPa}$, $G = 73.4 \text{ GPa}$. The sound velocities for khoharite at ambient conditions are then $V_p = 8.08 \text{ km/s}$ and $V_s = 4.36 \text{ km/s}$ (plotted in Fig. 5 as cyan squares). As seen in the figure, khoharite also has lower sound velocities compared to other silicate garnets, but occupies an intermediate position between andradite and skiaigite in the series of garnets with Y-site Fe^{3+} .

Skiaigite and khoharite are particularly relevant to the properties of Ca-depleted solid solutions. For instance, such garnets can be formed in harzburgite rock whose existence in the MTZ was proposed by Irifune et al. (2008). Indeed, the garnet inclusions from Xu et al. (2017) that contain a large proportion of khoharite have a low amount of CaO, but their genesis is unclear. In the following discussion, we will, therefore, consider only the inclusions from Kiseeva et al. (2017, accepted).

Influence of Y-site Fe^{3+} on sound velocities of garnet from MTZ

As a representative example of Y-site Fe^{3+} influence, we consider the JF-55A inclusion (formation depth of 440 km) with pyroxenitic composition from the Jagersfontein kimberlite (Kiseeva et al. 2017, accepted). This is the most oxidized garnet from the series, so it is ideal as a limiting case. Based on electron microprobe and Mössbauer data, the composition of JF-55A from single-crystal structure refinement is $(\text{Na}_{0.06}\text{Ca}_{0.57}\text{Fe}_{0.42}^{2+}\text{Mg}_{1.97})(\text{Al}_{1.01}\text{Fe}_{0.15}^{3+}\text{Si}_{0.44}\text{Mg}_{0.38})(\text{SiO}_4)_3$ (Kiseeva et al. 2017, accepted). Therefore, the endmember representation is 3% Na-maj + 38% Mg-maj + 27% Pyr + 13% Alm + 11.5% Gro + 7.5% And.

In the original publication, all iron was assumed to be ferrous in the reduction of electron microprobe data (Tapert et al. 2005). There is no unique chemical formula that can be written from these data. Indeed, it is impossible to derive a composition without excess cations or the presence of vacancies based on normal assumptions about site charges. To proceed, we consider the following end-member

representation: 3% Na-maj + 38% Mg-maj + 27% Pyr + 16% Alm + 16% Gro.

Using the experimentally determined unit cell parameter of JF-55A (Kiseeva et al. 2017, accepted), we obtain densities of 3.673 and 3.638 g/cm³ for the actual and “Fe²⁺ only” compositions, respectively. Elastic moduli and pressure derivatives of Mg-majorite were taken from Sinogeikin and Bass (2002). We neglect the Na-majorite contribution to the elastic moduli as there are no experimental data on the pressure derivative of its shear modulus. This term enters symmetrically in both representations, so it will not appreciably influence the relative difference between them.

The differences between the two representations are the amount of almandine and grossular, and the presence of andradite. From Fig. 5 one can see that consideration of Y-site Fe³⁺ should decrease the resulting sound velocities. Indeed, the calculations for composition with Fe³⁺ give $V_p = 8.88$ km/s and $V_s = 4.98$ km/s (Fig. 5), while for the “Fe²⁺ only” composition, the result is $V_p = 8.96$ km/s and $V_s = 5.03$ km/s at ambient conditions. Therefore, Y-site ferric iron decreases sound velocities by 1% in this case. At 20 GPa and 300 K, the difference remains 0.08 and 0.05 km/s for V_p and V_s , respectively. In terms of the 400–600 km depth interval in the preliminary reference Earth model (Dziewonski and Anderson 1981), it corresponds to a 16 km depth difference.

However, if instead of using the experimental unit cell parameter for both compositions, the values calculated using Vegard’s law are used [average unit cell parameters of Na- and Mg-majorite were taken from Bindi et al. (2011) and Angel et al. (1989), respectively], the difference in the velocities decreases to 0.05 and 0.03 km/s at ambient conditions for V_p and V_s , respectively. Moreover, the non-uniqueness of the “Fe²⁺ only” composition substantially spreads the range of this difference. We also note that current uncertainties in the determination of elastic moduli and their derivatives exceed such small differences. A striking example is the shear modulus of pyrope. In recent HPHT ultrasonic interferometry experiments in a multi-anvil press, the obtained values are 89.1(5) and 93.2(1) [Chantel et al. (2016) and Zou et al. (2012), respectively].

Conclusions

In this study, we performed an ambient temperature high-pressure NIS investigation of skiagite (77 mol%)–iron–majorite solid solution. The determined sound velocities are significantly lower than sound velocities of the silicate garnet end-members, grossular, pyrope, Mg-majorite, andradite, and almandine. We also estimated the sound velocities of two end-members with Fe³⁺ in the Y-site: skiagite and khoharite. Comparison of the

NIS-data-derived values of sound velocities with those estimated for pure skiagite demonstrates that the iron–majorite component decreases the sound velocities, especially V_s . The neglect of Y-site Fe³⁺ may decrease sound velocities of garnet solid solution relevant to MTZ up to 1% relative to a composition with only Fe²⁺ in the X-site.

Acknowledgements The authors are grateful to Dr. R. Mittal for the provided data. We thank the European Synchrotron Radiation Facility for the provision of synchrotron radiation (ID18). N.D. thanks the German Research Foundation (Deutsche Forschungsgemeinschaft, DFG, projects no. DU 954-8/1 and DU 95411/1) and the Federal Ministry of Education and Research, Germany (BMBF, grants no. 5K13WC3 and 5K16WC1) for financial support. C.M. and L.D. acknowledge DFG funding through projects MC 3–18/1 and MC 3–20/1 and the CarboPaT Research Unit FOR2125. Partial support was also provided by the German Academic Exchange Service (DAAD).

References

- Achterhold K, Keppler C, Ostermann A, Van B urck U, Sturhahn W, Alp E, Parak F (2002) Vibrational dynamics of myoglobin determined by the phonon-assisted M ossbauer effect. *Phys Rev E* 65(5):051916
- Angel R, Finger L, Hazen R, Kanzaki M, Weidner D, Liebermann R, Veblen D (1989) Letter. Structure and twinning of single-crystal MgSiO₃ garnet synthesized at 17 GPa and 1800  C. *Am Miner* 74(3–4):509–512
- Arimoto T, Gr eaux S, Irifune T, Zhou C, Higo Y (2015) Sound velocities of Fe₃Al₂Si₃O₁₂ almandine up to 19 GPa and 1700 K. *Phys Earth Planet Inter* 246:1–8
- Baima J, Ferrabone M, Orlando R, Erba A, Dovesi R (2016) Thermodynamics and phonon dispersion of pyrope and grossular silicate garnets from ab initio simulations. *Phys Chem Miner* 43(2):137–149
- Bindi L, Dymshits AM, Bobrov AV, Litasov KD, Shatskiy AF, Ohtani E, Litvin YA (2011) Letter. Crystal chemistry of sodium in the Earth’s interior: the structure of Na₂MgSi₃O₁₂ synthesized at 17.5 GPa and 1700  C. *Am Miner* 96(2–3):447–450
- Chantel J, Manthilake GM, Frost DJ, Beyer C, Ballaran TB, Jing Z, Wang Y (2016) Elastic wave velocities in polycrystalline Mg₃Al₂Si₃O₁₂-pyrope garnet to 24 GPa and 1300 K. *Am Miner* 101(4):991–997
- Chumakov A, R uffer R (1998) Nuclear inelastic scattering. *Hyperfine Interact* 113(1):59–79
- Dewaele A, Torrent M, Loubeyre P, Mezouar M (2008) Compression curves of transition metals in the Mbar range: experiments and projector augmented-wave calculations. *Phys Rev B* 78(10):104102
- Dziewonski AM, Anderson DL (1981) Preliminary reference Earth model. *Phys Earth Planet Inter* 25(4):297–356
- Erba A, Mahmoud A, Orlando R, Dovesi R (2014) Elastic properties of six silicate garnet end members from accurate ab initio simulations. *Phys Chem Miner* 41(2):151–160
- Gwanmesia GD, Wang L, Heady A, Liebermann RC (2014) Elasticity and sound velocities of polycrystalline grossular garnet (Ca₃Al₂Si₃O₁₂) at simultaneous high pressures and high temperatures. *Phys Earth Planet Inter* 228:80–87
- Hazen RM, Finger LW (1978) Crystal structures and compressibilities of pyrope and grossular to 60 kbar. *Am Miner* 63(3–4):297–303
- Hu M, Sturhahn W, Toellner T, Hession P, Sutter J, Alp E (1999) Data analysis for inelastic nuclear resonant absorption experiments. *Nucl Instrum Method Phys Res Sect A* 428(2):551–555

- Hu MY, Sturhahn W, Toellner TS, Mannheim PD, Brown DE, Zhao J, Alp EE (2003) Measuring velocity of sound with nuclear resonant inelastic X-ray scattering. *Phys Rev B* 67(9):094304
- Irifune T, Ringwood A (1993) Phase transformations in subducted oceanic crust and buoyancy relationships at depths of 600–800 km in the mantle. *Earth Planet Sci Lett* 117(1–2):101–110
- Irifune T, Sekine T, Ringwood A, Hibberson W (1986) The eclogite-garnetite transformation at high pressure and some geophysical implications. *Earth Planet Sci Lett* 77(2):245–256
- Irifune T, Higo Y, Inoue T, Kono Y, Ohfuji H, Funakoshi K (2008) Sound velocities of majorite garnet and the composition of the mantle transition region. *Nature* 451(7180):814–817
- Ismailova L, Bobrov A, Bykov M, Bykova E, Cerantola V, Kantor I, Kupenko I, McCammon C, Dyadkin V, Chernyshov D, Pascarelli S, Chumakov A, Dubrovinskaia N, Dubrovinsky L (2015) High-pressure synthesis of skiaegite-majorite garnet and investigation of its crystal structure. *Am Miner* 100(11–12):2650–2654
- Ismailova L, Bykov M, Bykova E, Bobrov A, Kupenko I, Cerantola V, Vasiukov D, Dubrovinskaia N, McCammon C, Hanfland M, Glazyrin K, Liermann HP, Chumakov A, Dubrovinsky L (2017) Effect of composition on compressibility of skiaegite-Fe-majorite garnet. *Am Miner* 102(1):184–191
- Jiang F, Speziale S, Shieh SR, Duffy TS (2004) Single-crystal elasticity of andradite garnet to 11 GPa. *J Phys Condens Matter* 16(14):S1041
- Kiseeva E, Vasiukov D, Wood B, McCammon C, Stachel T, Bykov M, Bykova E, Cerantola V, Chumakov A, Harris J, Dubrovinsky L (2017) Oxidised iron in garnets from the mantle transition zone. *Nat Geosci Rev* (accepted)
- Kohn V, Chumakov A (2000) DOS: Evaluation of phonon density of states from nuclear resonant inelastic absorption. *Hyperfine Interact* 125(1–4):205–221
- Kohn V, Chumakov A, Rüffer R (1998) Nuclear resonant inelastic absorption of synchrotron radiation in an anisotropic single crystal. *Phys Rev B* 58(13):8437
- Kono Y, Gréaux S, Higo Y, Ohfuji H, Irifune T (2010) Pressure and temperature dependences of elastic properties of grossular garnet up to 17 GPa and 1650 K. *J Earth Sci* 21(5):782–791
- Lacivita V, Erba A, Dovesi R, D'Arco P (2014) Elasticity of grossular–andradite solid solution: an ab initio investigation. *Phys Chem Chem Phys* 16(29):15331–15338
- Litasov KD, Ohtani E (2005) Phase relations in hydrous MORB at 18–28 GPa: implications for heterogeneity of the lower mantle. *Phys Earth Planet Inter* 150(4):239–263
- McCammon C, Ross N (2003) Crystal chemistry of ferric iron in (Mg,Fe)(Si,Al)O₃ majorite with implications for the transition zone. *Phys Chem Miner* 30(4):206–216
- Milman V, Akhmatkaya E, Nobes R, Winkler B, Pickard C, White J (2001) Systematic ab initio study of the compressibility of silicate garnets. *Acta Crystallogr Sect B Struct Sci* 57(2):163–177
- Mittal R, Chaplot S, Choudhury N, Loong CK (2000) Inelastic neutron scattering and lattice-dynamics studies of almandine Fe₃Al₂Si₃O₁₂. *Phys Rev B* 61(6):3983
- Mittal R, Chaplot S, Choudhury N (2001) Lattice dynamics calculations of the phonon spectra and thermodynamic properties of the aluminosilicate garnets pyrope, grossular, and spessartine M₃Al₂Si₃O₁₂ (M = Mg, Ca, and Mn). *Phys Rev B* 64(9):094302
- Momma K, Izumi F (2011) VESTA 3 for three-dimensional visualization of crystal, volumetric and morphology data. *J Appl Crystallogr* 44(6):1272–1276
- Papagelis K, Kanellis G, Ves S, Kourouklis G (2002) Lattice dynamical properties of the rare earth aluminum garnets (RE₃Al₅O₁₂). *Phys Status Solidi B* 233(1):134–150
- Ricolleau A, Perrillat JP, Fiquet G, Daniel I, Matas J, Addad A, Menguy N, Cardon H, Mezouar M, Guignot N (2010) Phase relations and equation of state of a natural MORB: implications for the density profile of subducted oceanic crust in the Earth's lower mantle. *J Geophys Res Solid Earth* 115(B8)
- Ringwood A (1991) Phase transformations and their bearing on the constitution and dynamics of the mantle. *Geochim Cosmochim Acta* 55(8):2083–2110
- Rodehorst U, Geiger CA, Armbruster T (2002) The crystal structures of grossular and spessartine between 100 and 600 K and the crystal chemistry of grossular-spessartine solid solutions. *Am Miner* 87(4):542–549
- Rohrbach A, Ballhaus C, Golla-Schindler U, Ulmer P, Kamenetsky VS, Kuzmin DV (2007) Metal saturation in the upper mantle. *Nature* 449(7161):456–458
- Rüffer R, Chumakov AI (1996) Nuclear resonance beamline at ESRF. *Hyperfine Interact* 97(1):589–604
- Sinogeikin SV, Bass JD (2002) Elasticity of majorite and a majorite-pyrope solid solution to high pressure: implications for the transition zone. *Geophys Res Lett* 29(2):4-1–4-4
- Sturhahn W, Chumakov A (1999) Lamb–Mössbauer factor and second-order Doppler shift from inelastic nuclear resonant absorption. *Hyperfine Interact* 123(1–4):809–824
- Sturhahn W, Jackson JM (2007) Geophysical applications of nuclear resonant spectroscopy. In: Ohtani E (ed) *Advances in high-pressure mineralogy*. Geological Society of America, Boulder, CO
- Tappert R, Stachel T, Harris JW, Muehlenbachs K, Ludwig T, Brey GP (2005) Diamonds from Jagersfontein (South Africa): messengers from the sublithospheric mantle. *Contrib Miner Petrol* 150(5):505–522
- Wood BJ, Kiseeva ES, Matzen AK (2013) Garnet in the Earth's mantle. *Elements* 9(6):421–426
- Woodland A, Koch M (2003) Variation in oxygen fugacity with depth in the upper mantle beneath the Kaapvaal craton, Southern Africa. *Earth Planet Sci Lett* 214(1):295–310
- Woodland AB, Ross CR (1994) A crystallographic and Mössbauer spectroscopy study of Fe₃²⁺Al₂Si₃O₁₂-Fe₃²⁺Fe₂³⁺Si₃O₁₂ (almandine–“skiaegite”) and Ca₃Fe₂³⁺Si₃O₁₂-Fe₃²⁺Fe₂³⁺Si₃O₁₂ (andradite–“skiaegite”) garnet solid solutions. *Phys Chem Miner* 21(3):117–132
- Woodland A, Angel R, Koch M, Kunz M, Miletich R (1999) Equations of state for Fe₃²⁺ Fe₂³⁺ Si₃O₁₂ “skiaegite” garnet and Fe₂SiO₄-Fe₃O₄ spinel solid solutions. *J Geophys Res Solid Earth* 104(B9):20049–20058
- Xu C, Kynický J, Tao R, Liu X, Zhang L, Pohanka M, Song W, Fei Y (2017) Recovery of an oxidized majorite inclusion from Earth's deep asthenosphere. *Sci Adv* 3(4):e1601589
- Zhou C, Gréaux S, Nishiyama N, Irifune T, Higo Y (2014) Sound velocities measurement on MgSiO₃ akimotoite at high pressures and high temperatures with simultaneous in situ X-ray diffraction and ultrasonic study. *Phys Earth Planet Inter* 228:97–105
- Zou Y, Irifune T, Gréaux S, Whitaker ML, Shinmei T, Ohfuji H, Negishi R, Higo Y (2012) Elasticity and sound velocities of polycrystalline Mg₃Al₂(SiO₄)₃ garnet up to 20 GPa and 1700 K. *J Appl Phys* 112(1):014910